scientific reports

Check for updates

OPEN

Experimental study on the influencing factors and pore production law of CO_2 huff-and-puff in tight sandstone reservoirs

Zhe Zhang[1], Jian Sun[1,2], Zhihao Niu[3], Zhilin Tuo[4], Xinyu Zhong[2], Xiaolei Zheng[5] & Rongjun Zhang[1,2]✉

In order to determine the influence of different factors on the CO_2 huff-and-puff displacement effect, a CO_2 huff-and-puff experiment was carried out with Chang 6 tight sandstone samples in Ordos Basin as the research object. Combined with nuclear magnetic resonance technology, the influences of injection pressure, cycle numbers and soaking time on the CO_2 huff-and-puff effect were evaluated, and the optimal CO_2 huff-and-puff parameters were optimized. The microscopic degree of crude oil production in different scale pores was quantitatively characterized. The results show that the injection pressure and the cycle numbers have a significant influence on the effect of CO_2 huff-and-puff. With the increase of injection pressure, huff-and-puff cycle numbers and soaking time, the recovery efficiency increases, but the growth range decreases. When the injection pressure is increased from 6 to 12MPa, the degree of pore mobilization in the oil in macro and medium pores (≥10ms) increases by 13.0%-22.63%. The recovery efficiency of a single round gradually decreased with the increase of huff-and-puff rounds. The first cycle of CO_2 huff-and-puff was the main contribution of crude oil recovery. However, the production effect of micro and small pores (<10ms) was significantly improved after multiple cycle numbers of CO_2 huff-and-puff. When the soaking time increases from 6 to 24h, the recovery efficiency increases by 11.47%-14.93%. After that, the influence of prolonged soaking time on the porosity production degree of cores with different permeability decreases. It is found that medium pores and macro pores are the main contributors to pore mobilization during multiple cycles of CO_2 huff-and-puff.

Keywords Tight sandstone reservoirs, Injection pressure, CO_2 huff-and-puff cycle numbers, Soaking time, Pore production law

With the decrease in conventional oil and gas resources, tight oil has become the hot spot of oil and gas exploration and development. The 2024 assessment conducted by the International Energy Agency (IEA) estimates that the remaining technically recoverable resources of global tight oil amount to approximately 734×10^9t.The United States, Russia, and China are among the world's leading countries in the field of tight oil exploration and development[1,2]. China is rich in tight oil and gas resources, with proven tight oil geological reserves of 7.37×10^8t, showing broad prospects for exploration and development[3–6]. However, the characteristics of complex pore structure, strong reservoir heterogeneity and generally low maturity pose greater challenges to the development of tight reservoirs[7]. At present, the development of tight reservoirs still mainly relies on multi-stage fracturing of horizontal Wells. However, the small pore throat, high seepage resistance, difficult water injection, and rapid production decline in the middle and late development of tight reservoirs lead to poor utilization of crude oil in pores and unsatisfactory development effect[8,9].

CO_2 flooding has become a prominent area of research due to its broad applicability, low cost of oil displacement, and ability to enhance oil recovery rates[10–12]. Compared to gases such as nitrogen and methane, CO_2 can achieve zero interfacial tension with crude oil within a smaller pressure range, as its minimum miscibility pressure is lower. Additionally, CO_2 demonstrates a greater propensity than water-phase fluids to

[1]School of Petroleum Engineering, Xi 'an Shiyou University, Xi'an, Shaanxi, China. [2]Xi'an Key Laboratory of Tight Oil (Shale Oil) Development (Xi'an Shiyou University), Xi'an, Shaanxi, China. [3]SINOPEC Northwest Oilfield Company, Luntai, Xinjiang, China. [4]PetroChina Changqing Oilfield Company, PetroChina, Gas Recovery Plant No.2, Yulin, China. [5]School of Earth Sciences and Engineering, Xi'an Shiyou University, Xi'an, Shaanxi, China. ✉email: rjzhang1105@163.com

penetrate tight reservoirs[13,14]. When mixed with crude oil, CO_2 reduces the oil's viscosity, significantly decreases seepage resistance, and expands the oil's volume, thereby enhancing its mobility and improving overall seepage efficiency[15–19].

Extensive research has been conducted on CO_2 huff-and-puff experiments to enhance the recovery of low-permeability reservoirs. Monger et al. demonstrated through laboratory and field tests that CO_2 huff-and-puff significantly increases the residual oil content in flooding light oil reservoirs[20]. Kovscek, Vega, and Gamadi, through CO_2 huff-and-puff depletion experiments, found that CO_2 effectively enhances oil recovery in tight reservoirs, highlighting molecular diffusion as the primary recovery mechanism[21,22]. Qian et al. evaluated injection pressure conditions, concluding that recovery rates are higher under near-miscible or miscible conditions without a significant increase in CO_2 gas sourcing costs [23]. Tang et al. investigated various injection-production methods and parameters, identifying injection timing as a critical factor influencing extraction rates and overall recovery. Their study proposed that CO_2 stimulation consists of four phases: CO_2 injection, oil and gas flowback, rapid oil production, and a decline in production rate, with flow dispersion and diffusion being the dominant recovery mechanisms[24].Song and Yu et al. analyzed the Bakken tight oil reservoir using indoor simulation experiments and numerical simulations, focusing on phase-change characteristics in the mass transfer process between CO_2 and formation crude oil. They also examined the effects of molecular diffusion, stimulation cycles, fracture length, and permeability on oil recovery, identifying molecular diffusion as a key factor in the production process[25,26]. Gao et al. compared the recovery performance of CO_2 in tight reservoirs under supercritical and non-supercritical conditions, quantitatively assessing the impact of injection volume, soaking time, and stimulation cycles on recovery. Their findings demonstrated that supercritical CO_2 significantly improves recovery in tight reservoirs[27]. Ma et al. analyzed the feasibility of CO_2 huff-and-puff in depleted tight reservoirs, concluding that this method markedly enhances recovery. They observed a significant increase in the gas-oil ratio after multiple huff-and-puff cycles, with smaller pore contributions dominating recovery during subsequent cycles[28].

Compared to low-permeability sandstone reservoirs, tight sandstone reservoirs are characterized by smaller pore throats, a higher prevalence of micro- and nano-scale pore throats, and greater microscopic heterogeneity[29–31]. Existing studies on CO_2 huff-and-puff flooding primarily focus on analyzing influencing factors and evaluating recovery efficiency, with relatively limited research on the micro-scale production behavior of crude oil in pores of different sizes. Based on this, this article Chang 6 tight sandstone reservoir in Ordos basin as the research object. CO_2 huff-and-puff flooding experiments were conducted using nuclear magnetic resonance (NMR) T_2 spectrum testing to evaluate the effects of injection pressure, soaking time, and cycle number on oil recovery. Optimal parameters were identified, and the pore-scale utilization characteristics of crude oil were quantitatively assessed. This work aims to provide a theoretical foundation for selecting effective oil recovery methods in tight sandstone reservoirs.

Evaluation basis of pore initiation law based on nuclear magnetic resonance technology

Nuclear magnetic resonance (NMR) means that hydrogen nuclei in a fluid are polarized and spin in a uniformly distributed static magnetic field, and resonance relaxation is generated under the action of a radio frequency (RF) field [32]. For tight reservoirs, the relaxation signal intensity of free fluids in pore media is much smaller than the surface relaxation of rock particles. The T_2 relaxation time formula can be simplified as follows(Equation 0.1) [27,28]:

$$\frac{1}{T_2} = \rho_M \frac{S}{V} \tag{1}$$

where S represents the internal surface area of rock pores; V represents the pore volume of rock; S/V represents the pore-specific surface of a rock; ρ_M denotes the pore surface relaxation strength constant. It can be seen that the NMR relaxation time T_2 reflects the pore size of the reservoir rock. The integral area contained in the T_2 spectrum curve and relaxation time axis is proportional to the pore fluid content, and the change of the integral area of the T_2 spectrum curve also represents the fluid production in the pore to a certain extent (Fig. 1). The effect of pore production can be expressed by the change degree of pore fluid cover before and after CO_2 huff-and-puff (Equation 0.2). In this study, $T_2 < 1$ms, $1\text{ms} \le T_2 < 10$ms, $10\text{ms} \le T_2 \le 100$ms and $T_2 > 100$ms were defined as micro pores, small pores, medium pores and macro pores.

$$R = \frac{S_0 - S_1}{S_0} \times 100\% \tag{2}$$

where R represents the degree of pore fluid production, S_0 is the integral area of the T_2 spectrum curve under saturated fluid conditions. S_1 is the integral area of the T_2 spectrum curve after the fluid in the pore is produced.

Experimental section

Materials

According to the formation water test results, the simulated formation water is configured, the water type is $CaCl_2$, and the salinity is 34000mg/L. Manganese chloride solution was used to shield the hydrogen signal, and the concentration of Mn^{2+} was 30000mg/L. The purity of the CO_2 gas source used in the experiment was 99.9%. The simulated crude oil used in the experiment is a mixture of stratum dehydrated crude oil and kerosene with a

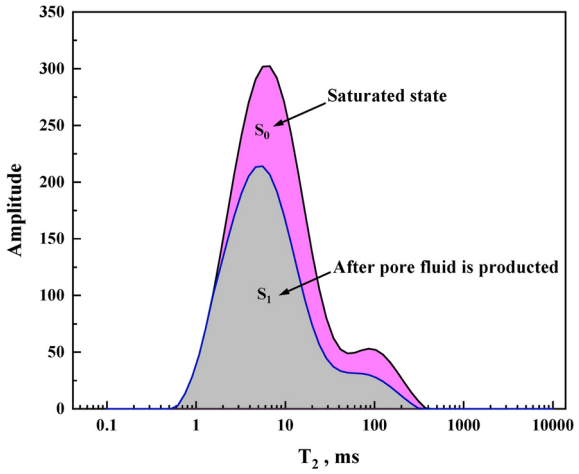

Fig. 1. T_2 spectrum before and after fluid production.

Sample No	Diameter(cm)	Length(cm)	Porosity(%)	permeability ($10^{-3}\mu m^2$)	Lithology
28	2.48	5.33	7.16	0.11	Sand
19	2.49	4.92	10.39	0.17	Sand
24	2.49	4.86	9.50	0.34	Sand

Table 1. Experimental sample information.

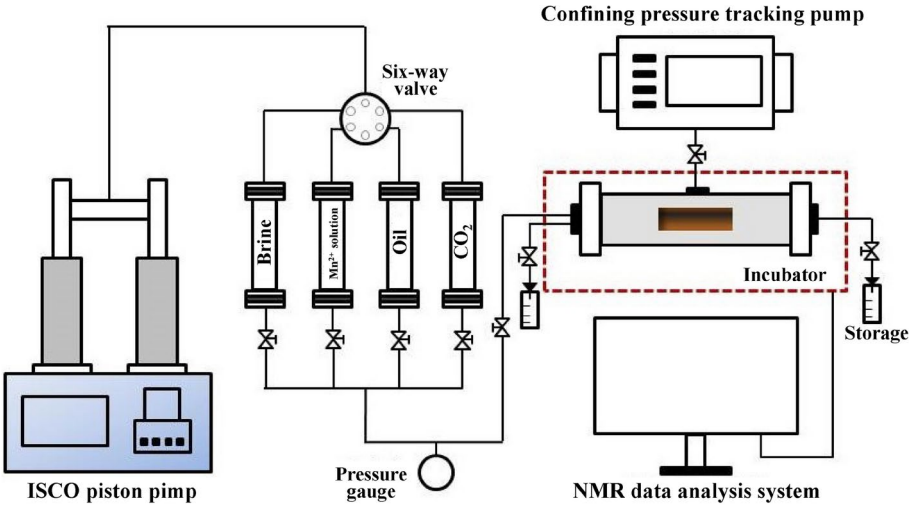

Fig. 2. Schematic diagram of CO_2 huff-and-puff experiment.

volume ratio of 1:3. Under the reservoir condition (8.88MPa, 40℃), the viscosity is 2.84 mPa·s, and the density is 0.861g/cm^3. Core samples were collected from Chang 6 tight sandstone reservoir in Yanchang, Ordos Basin. It is mainly composed of military arkose and the porosity of Core samples is between 7.16%-10.39%, and the permeability is $0.11 \times 10^{-3}\mu m^2$ and $0.34 \times 10^{-3}\mu m^2$, respectively (Table 1).

Experimental setup

The experimental equipment primarily includes an advection pump, a core gripper, an annular pressure tracking pump, a thermostat, and a nuclear magnetic resonance measuring instrument (Fig. 2). The constant-speed and constant-pressure pump (ISCO-500D, Xingke Company, China) operates at pressures ranging from 0 to 42.0 MPa, with parallel dual pump heads providing a maximum flow rate of 10.0 ml/min. The confining pressure tracking pump (Huaxing Company, China) has a maximum working pressure of 60 MPa and features real-time pressure tracking and rapid pressure compensation. The NMR equipment used is the Recore NMR sample

analyzer (Langfang, China), which operates at a magnetic field strength of 4.400 MHz. Key parameters include an echo time of 0.12 ms, an echo number of 5000, a measurement waiting time of 2500 ms, and 64 scanning cycles.

Experimental procedure

(1) Core samples were completely cleaned and placed in the incubator for drying, then measure their permeability.
(2) The brine was injected into the core sample steadily with a velocity of 0.10 mL/min before the amount of liquid produced is about 3 ~ 4PV, and the porosity and pore volume was calculated from the weight difference before and after saturation.
(3) To establish the initial oil–water distribution, the $MnCl_2$ aqueous solution was injected into the core sample steadily at the same rate.
(4) The crude oil was injected into the core sample with a velocity of 0.20 mL/min. The experiment was completed when the simulated crude oil was completely discharged from the outlet, and then measure the T_2 spectrum of the cores saturated with oil.
(5) The annular pressure tracking pump was activated, and its parameters were configured to maintain the annular pressure 2MPa above the injection pressure, ensuring full CO_2 entry into the core. The core holder outlet was then closed, and CO_2 was injected into the oil-saturated core at a constant pressure, which was incrementally set to 2, 4, 6, 8, 10, and 12MPa, until the pressure stabilized. After CO_2 injection, the soaking time was set to 12 h (t_{soak} = 12 h). After soaking, oil was produced from the same end of the core holder at atmospheric pressure. This process was repeated for subsequent cycles of the CO_2 huff-and-puff experiment until no more oil was recovered from the outlet. The core samples were then scanned to obtain the T_2 spectrum..
(6) To evaluate the displacement effects of CO_2 huff-and-puff under varying injection pressures, the results were compared, and the optimal injection pressure parameters were identified. Based on these parameters, the soaking time was varied to 6, 12, 24, 48, and 72h, and the process in step (5) was repeated.

Results and discussion

T_2 spectrum distribution of different core samples

The T_2 spectrum for the three oil-saturated core samples are shown in Fig. 3. A comparison indicated that the T_2 spectra of core samples No. 24 and No. 19 exhibited unimodal distributions, with relatively concentrated pore size distributions primarily in the medium and small pore intervals. The pore distribution frequency in medium pores was 86.47% for core sample No. 24 and 85.27% for core sample No. 19. In contrast, the T_2 spectrum of core sample No. 28 displayed a bimodal distribution, characterized by a wider distribution range and a higher content of micropores. Specifically, the pore distribution frequency for core sample No. 28 was 47.43% in small pores, 18.95% in medium pores, and 22.64% in micropores.

Influence of CO_2 huff-and-puff effect

Influence of injection pressure

According to the oil recovery of CO_2 huff-and-puff under different injection pressures (as shown in Fig. 4), the oil recovery of the three core samples exhibited distinct increasing trends with rising injection pressure. Core sample No. 24, having the highest permeability among the three, demonstrated a rapid increase in recovery efficiency at the early stage of pressure growth, achieving a higher recovery level at relatively low injection pressures. In contrast, core samples No. 19 and No. 28, with lower permeability, showed slower recovery increases at low injection pressures. However, as the injection pressure gradually increased, their oil recovery rose rapidly before stabilizing at higher pressures.

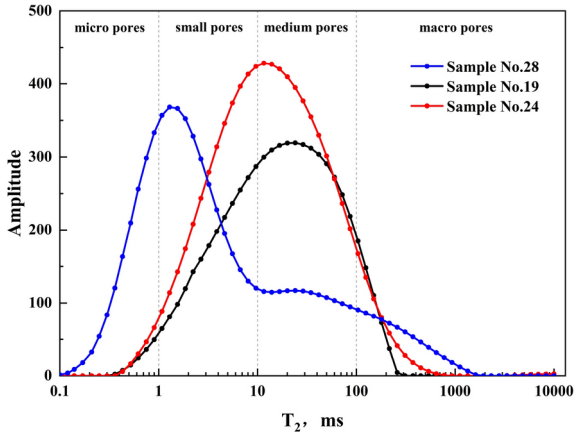

Fig. 3. T_2 spectrum of different core samples with oil saturated.

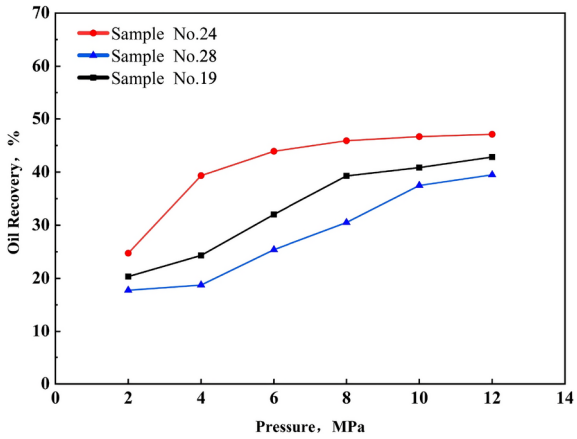

Fig. 4. Comparison of oil recovery under different injection pressure.

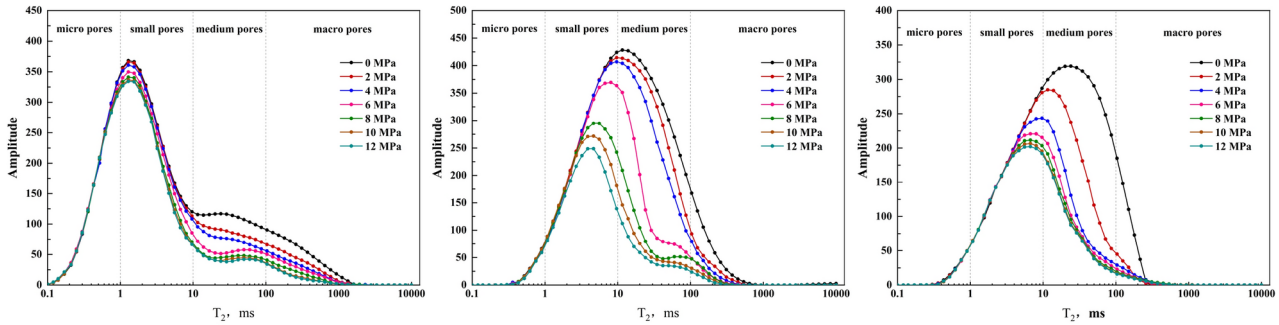

(a) Sample No.28 **(b) Sample No.19** **(c) Sample No.24**

Figure. 5. T_2 spectrum of the three cores under increasing injection pressure.

When the injection pressure increased from 2 to 6 MPa, the oil recovery efficiency of core sample No. 24 rose significantly from 24.73% to 44.51%. At injection pressures of 8 MPa, 10 MPa, and 12 MPa, the recovery efficiency increased to 45.89%, 46.65%, and 47.10%, respectively. For core sample No. 19, oil recovery efficiency increased from 20.34% to 39.24% when the pressure rose from 2 to 8 MPa, a total increase of 18.90%. However, further increasing the pressure to 12 MPa led to only a modest 3.56% improvement. Similarly, for core sample No. 28, oil recovery increased by only 0.97% when the pressure rose from 2 to 4 MPa. At 10 MPa, the recovery reached 37.49%, showing a period of rapid growth.

The analysis indicates that an optimal injection pressure exists in the CO_2 huff-and-puff process for tight sandstone reservoirs. The impact of increasing injection pressure on oil recovery efficiency was more pronounced in cores with lower permeability. Core sample No. 24, with the highest permeability, achieved a high recovery rate at a relatively low injection pressure of 6 MPa, while further pressure increases had a negligible effect. Conversely, in core samples No. 19 and No. 28, the lower permeability required the CO_2 to expend more energy to diffuse effectively and contact the oil in the pores. Significant recovery rates were achieved at 8 MPa and 10 MPa for these samples, respectively. Based on the experimental results, the optimal injection pressure values for core samples No. 28, No. 19, and No. 24 were determined to be 10 MPa, 8 MPa, and 6 MPa, respectively.

To investigate the differences in pore mobilization effects across various scales under different pressure conditions, a CO_2 huff-and-puff simulation experiment was conducted using T_2 spectrum analysis, with the results presented in Fig. 5. The T_2 spectrum curves for all three core samples decreased across different pore intervals as injection pressure increased, indicating varying degrees of oil displacement from the pores. However, significant reductions in the T_2 spectrum curve were primarily observed in medium and macro pores, with minimal changes in micro pores. Additionally, as the injection pressure increased, the decreasing trend in T_2 spectrum amplitude within the key pore regions became more pronounced.

For core sample No. 28, the T_2 spectrum signal amplitude did not change significantly overall. However, within the range of 11.58 ms to 1608.23 ms, the signal amplitude exhibited a notable decrease, indicating that oil displacement primarily occurred in the medium and macro pore regions. In core sample No. 19, the reduction in T_2 spectrum curve amplitude was concentrated in the large pore interval (1.29 ms to 774.26 ms), with negligible changes when the injection pressure was 4 MPa (Fig. 5b). As the injection pressure increased, the range of pore availability gradually shifted from large pores to medium and small pores, where oil utilization became increasingly dominant.

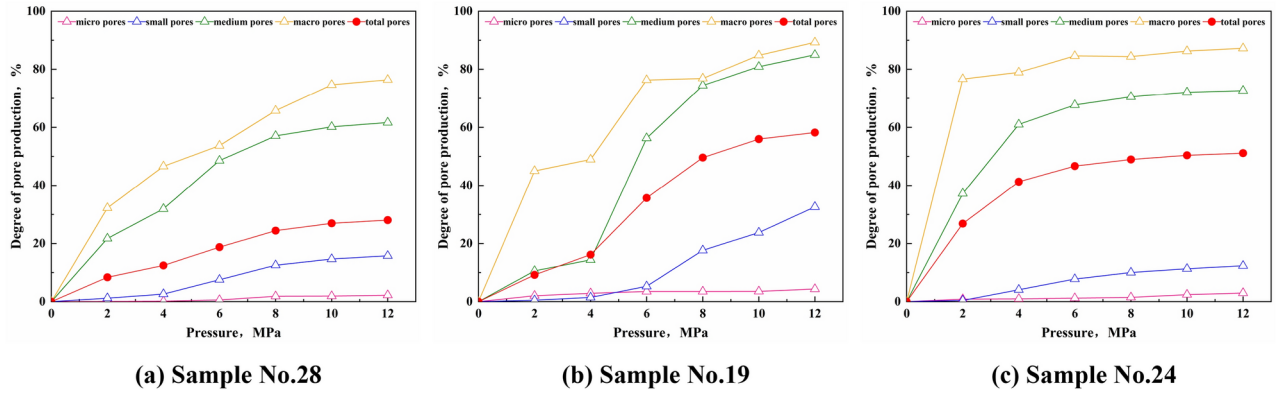

Figure. 6. The degree of pore production under different injection pressures.

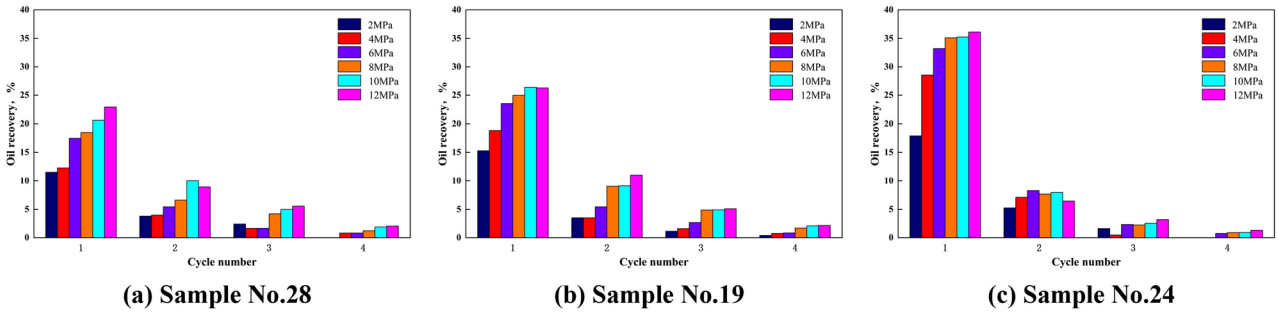

Figure. 7. Oil recovery under different cycle numbers.

Core sample No. 24 displayed similar pore mobilization patterns to core sample No. 19. However, a key difference was observed: When the injection pressure reached 6 MPa, the T_2 spectrum amplitude of core sample No. 24 did not decrease significantly. Instead, medium pores served as the primary interval for oil displacement in this core sample.

Figure 6 illustrates the variation in porosity mobilization across different scales as injection pressure increased during the CO_2 huff-and-puff process in cores with varying permeability. The results showed that porosity mobilization in all three core samples gradually increased with higher injection pressures. However, the trends of porosity mobilization across different scales varied significantly.In core sample No. 28, the mobilization of oil in macro and medium pores exhibited an early rapid increase followed by a slower growth phase. Oil production from small pores increased slightly with higher injection pressures but showed minimal overall growth. Due to the relatively high development of small and medium pores in this core, the overall degree of porosity mobilization remained relatively low.

For core sample No. 19, early-stage production was dominated by crude oil recovery from macro pores, with minimal contributions from small and medium pores. Once crude oil in the macro pores was depleted, oil in the medium pores redistributed, with some entering macro pores due to pressure differences. At this stage, oil mobilization in medium and small pores increased significantly. As injection pressure continued to rise, effective production from larger pores was observed.Core sample No. 24 exhibited different pore mobilization characteristics compared to the other cores. Early oil production from macro and medium pores reached a high level, but further growth was minimal with increasing pressure. The overall porosity mobilization curve closely mirrored the trend for macro and medium pores. Oil production from smaller pores showed only slow growth, indicating that porosity mobilization in core No. 24 was dominated by macro and medium pores. This behavior was attributed to the high degree of development of larger pores in the core.

Additionally, the degree of oil mobilization in micro pores was very low across all three cores, suggesting that increasing injection pressure had a limited effect on enhancing production from micro pores.

Influence of cycle numbers

In the actual development process, determining the optimal number of CO_2 stimulation cycles was crucial to achieving significant improvements in oil recovery. This was particularly important in tight sandstone reservoirs, where the efficiency of CO_2 huff-and-puff operations depended on the number of cycles performed. Since the optimal cycle count was not universally applicable across laboratory CO_2 huff-and-puff simulation experiments, this study investigated three core samples with varying permeability under multiple cycle numbers and injection pressures (ranging from 2 to 12 MPa). The relationship between oil recovery efficiency, system pressure variation, and cycle count was illustrated in Fig. 7.

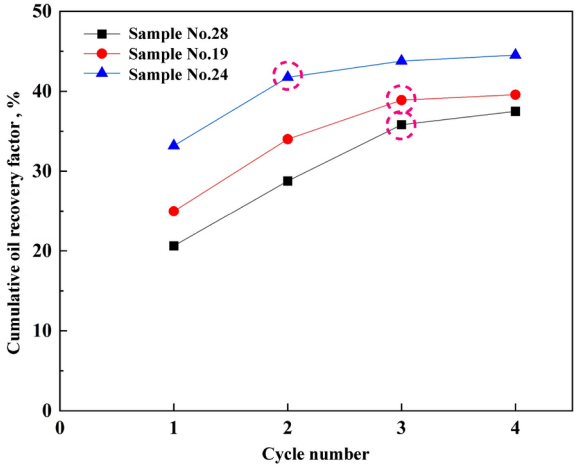

Figure. 8. Relationship between cumulative recovery and cycle under optimal injection pressure.

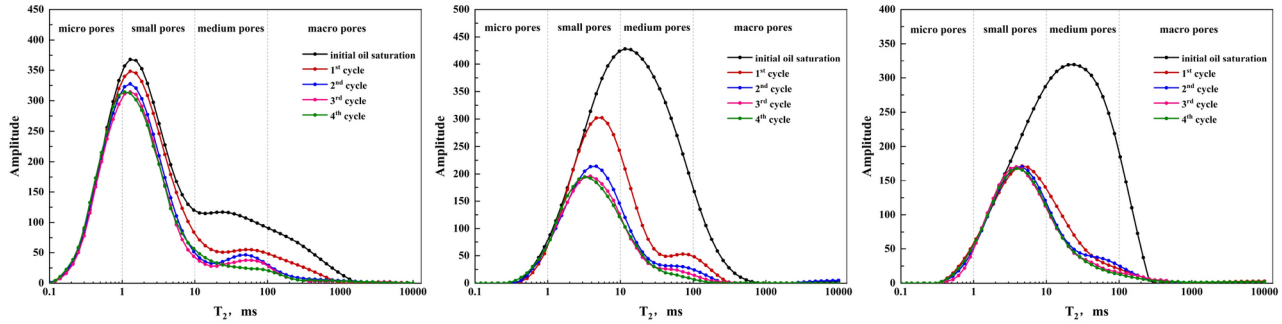

(a) Sample No.28 **(b) Sample No.19** **(c) Sample No.24**

Figure. 9. T_2 spectrum distribution of three core samples with increasing cycle numbers.

The results showed that under different injection pressures, oil recovery efficiency after each CO_2 stimulation cycle decreased as the number of cycles increased. For core sample No. 24, which had high permeability, the oil recovery rate after the first cycle was 36.13%, significantly higher than that of core sample No. 28 and core sample No. 19, which achieved recovery rates of 22.95% and 26.42%, respectively. However, the recovery performance of subsequent stimulation cycles in core sample No. 24 was notably weaker than in the other two samples. After the fourth cycle, the increase in oil recovery slowed considerably, indicating that minimal oil remained extractable from the pores.

As shown in Fig. 8, the cumulative recovery efficiency of the three core samples increased logarithmically with the number of cycles. However, the number of cycles required to reach the "cut-off point" of cumulative recovery growth varied depending on permeability. After four cycles, the cumulative recovery efficiency of the three core samples ranged from 37.49% to 44.51%. For core samples No. 28 and No. 19, the recovery efficiency of the first three cycles accounted for 82.17% and 84.58% of the total cumulative recovery, respectively, with increases of 12.92% and 10.55% after the second cycle of CO_2 huff-and-puff. In contrast, core sample No. 24 achieved a cumulative recovery factor of 41.74% after only two cycles, equivalent to 93.78% of its total recovery after four cycles.

Based on the above analysis, core sample No. 24, with high permeability, required only two cycles to achieve optimal throughput. In comparison, low-permeability cores (such as core samples No. 28 and No. 19) required additional cycles to enhance formation energy and mobilize oil from the denser matrix. Consequently, the optimal number of cycles for these low-permeability cores was determined to be three.

Figure 9 illustrates the variation in T_2 spectrum distribution for cores with different permeability as a function of cycle numbers. It was evident that with increasing cycle numbers, the T_2 spectrum curve shifted toward the left and downward, indicating that crude oil in the larger pore intervals was initially mobilized. However, after the second cycle, the decline in the T_2 spectrum curve across all pore intervals became less pronounced.

Core sample No. 28 exhibited two peaks in its T_2 spectrum, corresponding to two distinct types of pores: Small pores (0.1 ms to 13.89 ms) and large pores (13.89 ms to 1608.23 ms). As cycle numbers increased, oil in the large pores became the primary target for production. In contrast, the T_2 spectrum of core sample No. 19 initially covered a broad range, primarily reflecting the mobilization of oil in medium pores. With additional cycles, crude oil in the medium pores became dominant, and after the second cycle, the T_2 spectrum curve

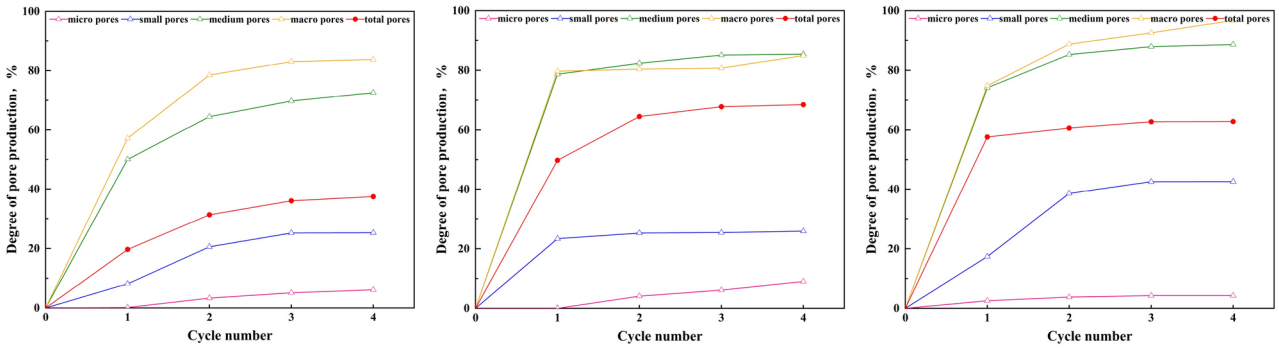

(a) Sample No.28 (b) Sample No.19 (c) Sample No.24

Figure. 10. The degree of pore production under different cycle numbers.

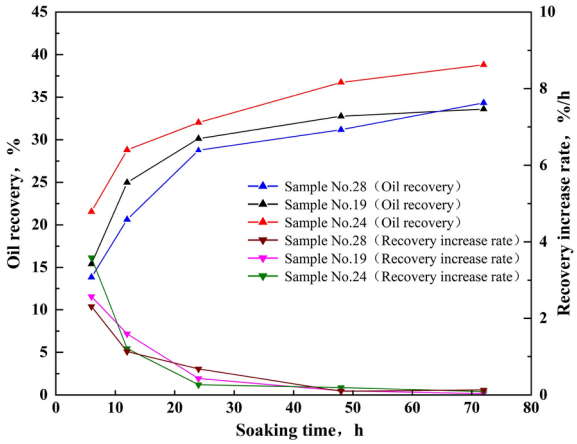

Figure. 11. Relationship between oil recovery, recovery increase rate, and soaking time of three core samples.

declined only in the small and medium pore intervals. Core No. 24 displayed a different trend. After the first cycle, its T_2 spectrum curve showed a significant decline in large pores (1.29 ms to 774.26 ms). The decline was relatively pronounced during the first cycle but became notably smaller in subsequent cycles. Moreover, after the second cycle, the T_2 spectrum curve in the medium pores increased rather than decreased, suggesting that oil and water were redistributed. This redistribution allowed oil to re-enter previously utilized pores under the influence of pressure differences.

Figure 10 shows the variation in pore production across different scales with increasing cycle numbers during the CO_2 huff-and-puff process in cores with varying permeability. The production levels of macro and medium pores in all three cores reached a high level after the first and second cycles, with the growth rate of pore production slowing as cycle numbers increased. The total pore production curves for the three cores exhibited a similar trend; however, core sample No. 28, characterized by a high content of fine pores, demonstrated the lowest overall pore production efficiency. Specifically, the total pore production for the four cycles was 19.65%, 31.32%, 36.04%, and 37.47%, respectively.

In the early stages, the pore production levels of macro, medium, and small pores in core sample No. 19 increased rapidly before plateauing. However, the second cycle significantly enhanced pore production in the micro pores of core sample No. 19, leading to a continued increase in the total pore production curve after the first cycle. The total pore production for the four cycles was 49.75%, 64.45%, 67.77%, and 68.45%, respectively.

For core sample No. 24, an initial rapid increase in the utilization of larger pore intervals was observed, followed by a deceleration in the growth rate. This indicates that increasing stimulation cycles facilitated deeper extraction of remaining movable oil within the pore throats of tight reservoirs. However, as shown in Fig. 10(c), further increases in pore production within specific intervals did not significantly enhance the overall production. The oil displacement and recovery effects of CO_2 stimulation were predominantly reflected in the production of larger pores. The total pore production for four stimulation cycles was 57.60%, 60.58%, 62.69%, and 62.75%, respectively.

Influence of soaking time

Figure 11 illustrates the relationship between the recovery efficiency of three core samples and the soaking time. When the soaking time increased from 6 to 24 h, the recovery efficiency rose significantly. However, with a

further increase in soaking time, the rate of recovery efficiency growth gradually diminished. For core samples No. 19 and No. 28, the recovery efficiency at 24 h improved substantially, increasing by 14.72% and 14.93%, respectively, compared to 6 h. In contrast, the recovery efficiency of core sample No. 24 was 21.55% after 6 h of soaking but grew slowly with an extended soaking time to 24 h. Ultimately, after 24 h, the recovery efficiency reached only 32.02%, indicating that CO_2 effectively reacted with crude oil in low-permeability cores within a relatively short time frame.

When the soaking time extended from 24 to 72 h, the recovery efficiency of core samples No. 19 and No. 28 increased by only 3.47% and 5.57%, respectively. In contrast, the recovery efficiency of core sample No. 24 increased by 17.26% compared to its initial recovery after 72 h of soaking. This suggests that prolonged soaking time significantly enhanced the oil displacement effect in high-permeability cores.

To further investigate the effect of soaking time on CO_2 huff-and-puff performance, the concept of the recovery increase rate (RIR) was introduced. RIR is defined as the ratio of the recovery increment of CO_2 huff-and-puff to the corresponding soaking time increment under the same experimental conditions. Figure 11 shows that all three core samples exhibited varying degrees of decline in RIR during prolonged soaking, with RIR inversely proportional to soaking time. At 12 h, the RIR of core sample No. 24 rapidly increased to 1.21%/h. However, the RIR of core samples No. 19 and No. 28 declined significantly at 24 h, ultimately decreasing by 2.53%/h and 2.18%/h, respectively, compared to their initial RIR values. By 24 h, the RIR of all three core samples had dropped below 1.00%/h per cycle. Analysis of the recovery curves indicated that the optimal soaking time was 48 h for core sample No. 24 and 24 h for core samples No. 19 and No. 28.

The relationship between the T_2 spectrum of core samples and soaking time is presented in Fig. 12. With increasing soaking time, the T_2 spectrum distribution curves of the three core samples exhibited varying degrees of decline across pores of different scales. The decline was more pronounced after 24 h of soaking but became less significant thereafter. A comparison revealed that the T_2 spectrum curve of core sample No. 28 showed minimal variation, as oil in the small pores (left peak) and most large pores (right peak) was effectively utilized during the early soaking stages. Beyond 24 h, the decrease in the T_2 spectrum of medium and macro pores was more significant than that of small pores; however, extending the soaking time had little additional impact on oil production from any pore size.For core sample No. 19, changes in the T_2 spectrum curve during the early soaking stage (12 h) primarily occurred in medium and macro pores. As soaking time increased, production shifted from medium and macro pores to small pores, with the production range gradually decreasing. In contrast to the other two cores, core sample No. 24 exhibited a wider range of variation in its T_2 spectrum curve, though the largest decreases were observed in the medium pores. Even after prolonged soaking, small decreases in the T_2 spectrum curve were still observed in the micro and small pores.

Figure 13 further illustrates the variation in pore production across different scales with increased soaking time during CO_2 huff-and-puff in cores of varying permeability. The pore production degree of the three cores rose rapidly with extended soaking time during the initial stage but slowed gradually thereafter. After prolonged soaking, the production effect of medium and macro pores was superior to that of micro and small pores across all core samples. In the early stages for core sample No. 28, crude oil was predominantly produced from medium and large pores, with minimal production from micro pores. After 24 h of soaking, the overall pore production effect diminished with further soaking. In core sample No. 19, the production degree of medium and macro pores was consistently the highest, followed by small pores, with micro pores beginning production only after 24 h of soaking. Core sample No. 24 exhibited distinct characteristics: Macro pores achieved high production levels early in the soaking process, and the total pore production curve mirrored this trend, reflecting the high content of large pores in the sample.

Conclusion

(1) Injection pressure and cycle numbers significantly influence the effectiveness of CO_2 huff-and-puff in enhancing oil recovery. As injection pressure and cycle numbers increase, oil recovery also improves; however, the incremental growth rate gradually diminishes. When the injection pressure rises from 4 to 10 MPa, the recovery increment ranges from 10.50% to 18.76%. The average contribution to recovery from the third

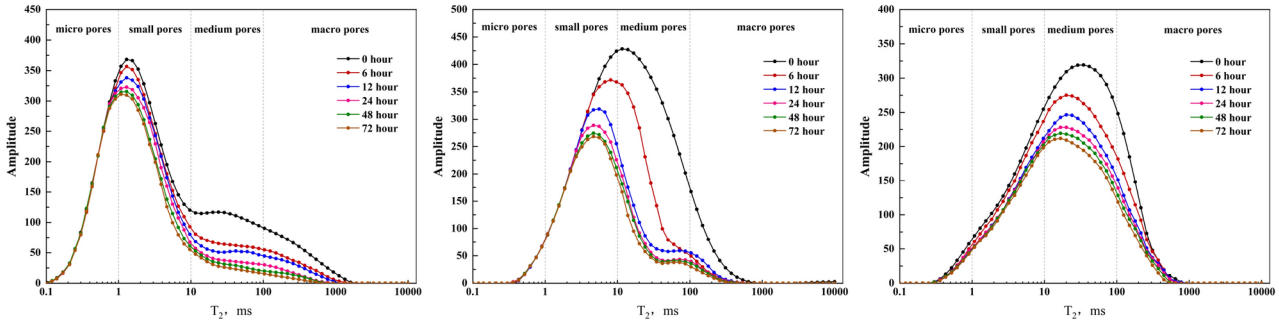

(a) Sample No.28 **(b) Sample No.19** **(c) Sample No.24**

Figure. 12. T_2 spectrum distribution of three core samples under different soaking time.

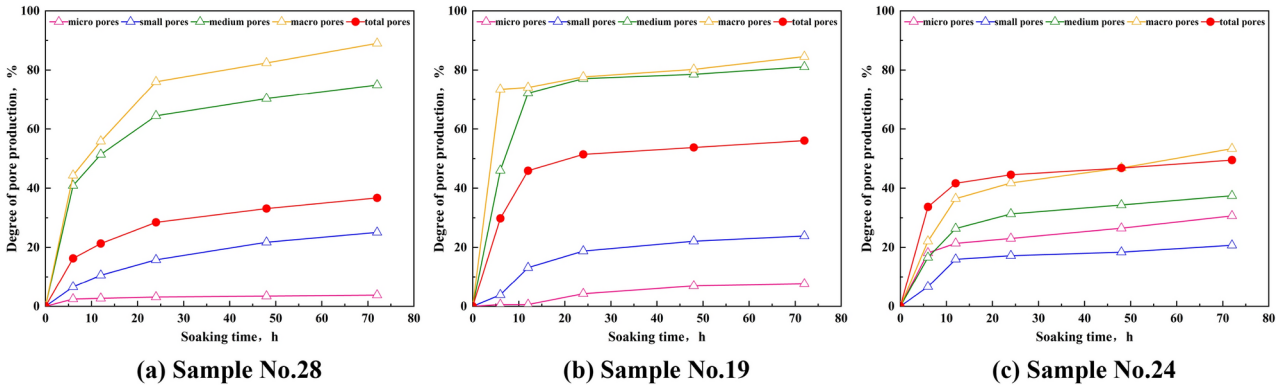

Figure. 13. The degree of pore production under different soaking time.

and fourth huff-and-puff cycles for 6.37% to 15.25%. Cores with lower permeability demonstrate a more pronounced improvement in recovery efficiency due to increased injection pressure and cycle numbers.

(2) When the soaking time is extended to 72 h, core samples No.19 and No.28 exhibit recovery increases of only 3.47% and 5.57%, respectively, compared to the recovery after 24 h of soaking. In contrast, core sample No. 24 achieves a more substantial increase of 6.79%. Low-permeability cores achieve rapid recovery improvements within relatively short soaking durations, while high-permeability cores require extending the soaking time appropriately to enhance oil recovery.

(3) The degree of pore utilization exhibits substantial variation under different influencing factors, with medium-to-large pores being the dominant contributors to pore mobilization, achieving utilization rates between 37.45% and 96.69%. Repeated cycles of CO_2 huff-and-puff demonstrate distinct impacts on pore utilization characteristics across cores with varying permeabilities. Higher permeability correlates with a more concentrated pore size distribution and greater mobilization efficiency in micro-to-small pores ($T_2 < 10$ ms). In the early stages of well soaking, crude oil mobilization within the pores is significantly affected; however, prolonging the soaking duration enhances the mobilization efficiency of micropores in cores with higher permeability.

Data availability statement

Data is provided within the manuscript or supplementary information files.

Received: 23 October 2024; Accepted: 22 January 2025
Published online: 28 January 2025

References

1. Fangzheng, J. I. A. O. Re-recognition of "unconventional" in unconventional oil and gas. *Pet. Explor. Dev.* **46**(5), 803–810 (2019).
2. Global Energy and Climate Model - Analysis. IEA, www.iea.org/reports/global-energy-and-climate-model.
3. Caineng, Z. O. U. et al. Formation, distribution, potential and prediction of global conventional and unconventional hydrocarbon resources. *Pet. Explor. Dev. Online* **42**(1), 14–28 (2015).
4. Longde, S. U. N. et al. Development characteristics and orientation of tight oil and gas in China. *Pet. Explor. Dev.* **46**(06), 1073–1087 (2019).
5. Wenzhi, Z. H. A. O. et al. Types and resource potential of continental shale oil in China and its boundary with tight oil. *Pet. Explor. Dev. Online* **47**(1), 1–11 (2020).
6. Xiaomin, Z. H. U. et al. Research progress and core issues in tight reservoir exploration. *Earth Sci. Front.* **25**(02), 141–146 (2018).
7. Gao, H. & Li, H. Determination of movable fluid percentage and movable fluid porosity in ultra-low permeability sandstone using nuclear magnetic resonance (NMR) technique. *J. Pet. Sci. Eng.* **133**, 258–267 (2015).
8. Weiyao, Z. H. U. et al. Research progress on tight oil exploration in China. *Chin. J. Eng.* **41**(09), 1103–1114 (2019).
9. Wang, L. et al. Advances in improved/enhanced oil recovery technologies for tight and shale reservoirs. *Fuel* **210**, 425–445 (2017).
10. Martin, D. F. et al. Carbon dioxide flooding. *J. Pet.Technol.* **44**(04), 396–400 (1992).
11. Shu, C. H. E. N. et al. Prospects and key scientific issues of CO2 near-miscible flooding. *Pet. Sci. Bull.* **5**(03), 392–401 (2020).
12. Wang, Q. et al. Effect of a pore throat microstructure on miscible CO_2 soaking alternating gas flooding of tight sandstone reservoirs. *Energy Fuels* **34**(8), 9450–9462 (2020).
13. Brownstein, K. R. & Tarr, C. E. Importance of classical diffusion in NMR studies of water in biological cells. *Phy. Rev. A.* **19**(6), 2446–2453 (1979).
14. Zuloaga, P. et al. Performance evaluation of CO_2 Huff-n-Puff and continuous CO_2 injection in tight oil reservoirs. *Energy* **134**, 181–192 (2017).
15. Lei, H. et al. Oil recovery performance and CO_2 storage potential of CO_2 water-alternating-gas injection after continuous CO_2 injection in a multilayer formation. *Energy fuels* **30**(11), 8922–8931 (2016).
16. Beliveau, D., Payne, D. A. & Mundry, M. Waterflood and CO_2 flood of the fractured midale field. *J. Pet. Technol.* **45**(09), 881–817 (1993).
17. Chen, C. & Gu, M. Investigation of cyclic CO_2 huff-and-puff recovery in shale oil reservoirs using reservoir simulation and sensitivity analysis. *Fuel* **188**, 102–111 (2017).
18. Chen, C., Balhoff, M. & Mohanty, K. K. Effect of reservoir heterogeneity on primary recovery and CO_2 huff -n-puff recovery in shale-oil reservoirs. *SPE Reserv. Eval. Eng.* **17**(03), 404–413 (2014).
19. Koorosh, A.; Farshid, T. Laboratory Experimental Results of Huff-and-Puff CO_2 Flooding in a Fractured Core System, In *SPE Annual Technical Conference and Exhibition* (Anaheim, California, USA, 2007)

20. Monger, T. G. & Coma, J. M. A laboratory and field evaluation of the co$_2$ huff-n-puff process for light-oil recovery. *Spe. Reserv. Eng.* **3**(04), 1168–1176 (1988).
21. Vega B , ,Kovscek A R . Experimental investigation of oil recovery from siliceous shale by miscible CO_2 injection.In. *SPE135627* (2010).
22. Gamadi T D, ShengJJ, Solian M Y, et al. An experimental study of Cyclic CO_2 Injection to Improve shale oil recovery.In. *SPE169142* (2014).
23. Qian, K. et al. Experimental investigation on microscopic residual oil distribution during CO_2 Huff-and-Puff process in tight oil reservoirs. *Energies* **11**(10), 2843 (2018).
24. Xiang, T. A. N. G. et al. Dynamic characteristics and influencing factors of CO2 huff and puff in tight oil reservoirs. *Pet. Explor. Dev.* **48**(04), 946–955 (2021).
25. Song, C. & Yang, D. Experimental and numerical evaluation of CO_2 huff-n-puff processes in Bakken formation. *Fuel* **190**, 145–162 (2017).
26. Yu W, Lashgari H R, Sepehrnoori K. Simulation Study of CO_2 Huff-n-Puff Process in Bakken Tight Oil Reservoirs. In *SPE Western North American and Rocky Mountain Joint Meeting*. OnePetro (2014).
27. Gao, H. & Pu, W. Experimental study on supercritical CO_2 huff and puff in tight conglomerate reservoirs. *ACS omega* **6**(38), 24545–24552 (2021).
28. Quanzheng, M. A. et al. Effect and influencing factors of CO_2 huff and puff in a tight oil reservoir——Taking the Lucaogou formation in the Xinjiang Jimsar sag as an example. *Pet. Sci. Bull.* **3**(04), 434–445 (2018).
29. Song, Y. et al. Magnetic resonance imaging study on near miscible supercritical CO_2 flooding in porous media. *Phy. Fluid.* **25**(5), 053301 (2013).
30. Gao, H. et al. Quantitative study on the stress sensitivity of pores in tight sandstone reservoirs of Ordos basin using NMR technique. *J. Pet. Sci. Eng.* **172**, 401–410 (2019).
31. Gao, H. et al. Comprehensive characterization of nano-pore system for chang 7 shale oil reservoir in ordos basin. *Energy Explor. Exploit.* **39**(1), 180–200 (2021).
32. Hui, G. A. O. et al. Application of NMR technique in evaluation of micro-pore structure in extra-low permeability sandstone. *Prog. Geophy.* **26**(01), 294–299 (2011).

Acknowledgements

This work has been supported jointly by the Key Research and Development Program of Shaanxi Province (Grant No. 2021KW-10), Shaanxi Province Science and Technology Re-sources Open Sharing Platform Project（Grant No.2022PT-08），The National Natural Science Foundation of China（Grant No.52304036）。

Author contributions

Z.Z., J.S. and X.Z.carried out the experiments. Z.N. and Z.T. provided the experimental set-up and some of the materials. R.Z., Z.Z., J.S., X.Z., and X.Z. contributed to the analysis of enhanced oil recovery calculations. R.Z., Z.Z. and X.Z. analysed the experimental results. Z.Z. and J.S. wrote the manuscript. R.Z., Z.N. and Z.T. designed the project. Z.Z. and J.S. conceived the ideas. R.Z and Z.T. supervised the project.

Declarations

Competing interests

The authors declare no competing interests.

Additional information

Data is provided within the manuscript or supplementary information files.

Additional information

Supplementary Information The online version contains supplementary material available at https://doi.org/10.1038/s41598-025-87846-3.

Correspondence and requests for materials should be addressed to R.Z.

Reprints and permissions information is available at www.nature.com/reprints.

Publisher's note Springer Nature remains neutral with regard to jurisdictional claims in published maps and institutional affiliations.